


## Generation of Bures-Hall mixed states using coupled kicked tops

Ayana Sarkar\* and Santosh Kumar†

*Department of Physics, Shiv Nadar University, Gautam Buddha Nagar, Uttar Pradesh 201314, India*
 (Received 15 August 2020; revised 14 January 2021; accepted 1 March 2021; published 18 March 2021)

We simulate a system of coupled kicked tops to generate random density matrices distributed according to the Bures-Hall measure, which has an important role in quantum information theory. We study the effects of stochasticity and coupling parameters of the coupled-kicked-top system on the behavior of the associated bipartite pure state, eigenvalues and eigenvectors of the reduced state, and average entropies. For strongly chaotic phase space and adequate coupling between the constituting tops (subsystems), we find that the results of simulation agree with analytical results of random matrix theory. We also examine local fluctuation properties of the Bures-Hall eigenvalues using the distribution of nearest-neighbor spacing ratios. In the limit of high-dimensional density matrices, the empirical ratio distribution is found to approach the Wigner-surmise-like result for the Gaussian unitary ensemble. Additionally, we present some closed-form results for the Bures-Hall spectral density and corresponding moments using Meijer  $G$  functions.

DOI: [10.1103/PhysRevA.103.032423](https://doi.org/10.1103/PhysRevA.103.032423)

### I. INTRODUCTION

In recent times, the investigation of statistical properties of random quantum states has garnered a lot of attention due to a plethora of applications in quantum computation and quantum information theory [1,2]. Random quantum states correspond to minimal prior knowledge about a system and provide the most typical or generic description [3,4]. Another major motivation in studying random states comes from quantum chaos, where it is often important to judge whether a given state whose classical analog is chaotic is effectively random [5–7]. They also serve as a reference for the arbitrary time evolution of initial states of quantum analogs of classically chaotic systems [6].

Random states may be classified into two types: pure and mixed states. A pure state of a quantum system, defined on Hilbert space, is represented by the state vector  $|\psi\rangle$ . A random pure state may be generated using the Haar measure [3]. The density-matrix approach is an alternative formalism to the state-vector representation and is indispensable for defining mixed states. Unlike pure states, mixed states have no single unique measure which can describe their statistics. Two foremost choices of measure on the set of finite-dimensional density matrices describing mixed states are the Hilbert-Schmidt (HS) and Bures-Hall (BH) measures [8,9]. The HS measure corresponds to the fixed-trace Wishart ensemble and has been studied exhaustively in random matrix theory (RMT) [10–34]. The corresponding unrestricted-trace variant is already well known in the field of multivariate statistics [35–41] and is related to the fixed-trace variant via a Fourier-Laplace transform. In contrast, within RMT, the BH measure

has been explored very little due to its complexity [3,4,8,9,42–52].

The BH measure exhibits some very interesting mathematical properties and plays a crucial role in quantum information theory [44,45,53–58]. For instance, in quantum state estimation and tomographic applications, the BH measure is used as a prior in the Bayesian approach [59–62]. A simple and efficient algorithm to generate BH-distributed random states is known due to Życzkowski and coworkers [46]. In its standard form, the BH measure results from the Bures distance metric by assigning equal masses to balls of equal radii [4,8]. The Bures metric is associated with *fidelity*, which is a common measure of efficiency in quantum state estimation and has been discussed at length in the context of quantum information and quantum computation in Refs. [1,63–67]. Other important applications of the Bures metric are in quantum metrology [68] and in defining a geometric discord to measure quantum correlations [69–78]. *Fidelity decay* has also been established as an efficient indicator of quantum chaos in quantum information processing systems [79].

A generalization of the standard BH measure is obtained by considering the partial-trace operation on a pure state of larger dimension [3,44,46], as discussed below. This gives an additional parameter in the induced BH measure which relates to the Hilbert-space dimension of the *environment* [44,50,51]. This more general ensemble has been the subject of very recent investigations which have resulted in exact analytical results pertaining to its spectrum and the associated entropies [50,80,81]. In the present work, for brevity, we refer to this generalized ensemble also as the BH ensemble.

It is known that universal correspondence between the spectral statistics of quantized classical systems and canonical random matrix ensembles is the most popular signature of quantum chaos. This provides us another motivation to study the Bures-Hall measure and the associated random states in the context of RMT and quantum chaos. Kicked

\*ayana1994s@gmail.com

†skumar.physics@gmail.com

tops have been standard models [7,82–86] in the investigation of quantum chaos and entanglement production in coupled chaotic systems [87–96]. In particular, the rate of dynamical generation of entanglement, entanglement content among the subsystems of the composite bipartite system, and the global entangling power have been studied by varying the stochasticity and coupling parameters of the coupled-kicked-top system [89,97–103]. Remarkably, kicked tops have also been realized experimentally using an ensemble of laser-cooled cesium atoms [88]. Statistical properties of the HS ensemble and the corresponding Schmidt eigenvalues have been well explored via coupled kicked tops [32,33,101,104–108]. However, similar studies have been missing so far for the BH measure.

Our objective in this paper is to fill this gap, and we aim to generate BH distributed reduced density matrices using the coupled-kicked-top system. We examine the behavior of the bipartite pure states generated in the coupled-kicked-top simulation. Afterwards, for the reduced state obtained by the partial-trace operation, we study the statistics of eigenvalues and eigenvectors. We investigate the dependence of these quantities and the related average entropies on the stochasticity and coupling parameters of the coupled-kicked-top system. The observations from the simulations are compared with the RMT analytical results, and thereby suitable parameter values are ascertained which result in the coupled-kicked-top reduced state mimicking a BH-distributed state. In this connection, we also provide some analytical results for the spectral density and moments of BH eigenvalues. Additionally, we focus on the local fluctuation properties of the BH spectrum and evaluate the ratios of consecutive level spacings [109–122]. In the high-dimension limit, we contrast it with the Wigner-surmise-like results for the Gaussian unitary ensemble (GUE) of random matrices [109] to examine possible universal behavior.

The presentation scheme for the rest of this paper is as follows. In Sec. II we briefly describe the BH measure and the corresponding RMT model. In Sec. III we collect necessary analytical results for comparison with coupled-kicked-top simulations carried out below. These include closed-form expressions for the spectral density and the associated moments of BH-distributed density matrices. In Sec. IV, we describe the algorithm for generating the desired random density matrices using coupled kicked tops. The simulation results are presented in Sec. V and compared with the analytical results. We conclude with a brief summary of the results and point out the future prospects in Sec. VI.

## II. THE BURES-HALL MEASURE

The BH-distributed random states are constructed by the reduction of a superposition of a random bipartite pure state and its local unitarily transformed copy [3,46], as described below. Consider a random pure state  $|\psi\rangle$  defined with the aid of Haar measure and belonging to a bipartite composite  $nm$ -dimensional Hilbert space  $\mathcal{H}_A^{(n)} \otimes \mathcal{H}_B^{(m)}$ . Here,  $\mathcal{H}_A^{(n)}$  and  $\mathcal{H}_B^{(m)}$  are  $n$ - and  $m$ -dimensional ( $m \geq n$ ), respectively.  $\mathcal{H}_A$  may be interpreted as representing a system, and  $\mathcal{H}_B$  may be interpreted as the environment. Now, let  $|\tilde{\psi}\rangle$  be the state  $|\psi\rangle$  transformed by a local  $n$ -dimensional unitary matrix  $U$ , i.e.,  $|\tilde{\psi}\rangle = (U \otimes \mathbb{1}_m)|\psi\rangle$ . This unitary matrix  $U$  is taken from the

measure given by  $|\det(\mathbb{1}_n + U)|^{2(m-n)}d\mu(U)$ , with  $d\mu(U)$  being the Haar measure on the set of  $n$ -dimensional unitary matrices [50,51]. Reducing the superposition  $|\vartheta\rangle = (|\psi\rangle + |\tilde{\psi}\rangle) = (\mathbb{1}_{nm} + U \otimes \mathbb{1}_m)|\psi\rangle$  via partial tracing over subsystem  $B$  (the environment), one gets the  $n$ -dimensional reduced density matrix,

$$\rho = \frac{\text{Tr}_B(|\vartheta\rangle\langle\vartheta|)}{\langle\vartheta|\vartheta\rangle}. \tag{1}$$

Here,  $\text{Tr}_B$  denotes partial tracing over subsystem  $B$ . The reduced density matrix  $\rho$  constructed in the above manner belongs to the BH measure, which is governed by the probability density [3,44,46],

$$\mathcal{P}_{\text{BH}}(\rho) \propto \delta(\text{Tr}\rho - 1) \frac{(\det \rho)^\alpha}{\prod_{j>k} (\mu_j + \mu_k)} \Theta(\rho), \tag{2}$$

where  $\alpha = m - n - 1/2$ . The Dirac delta function  $\delta(\text{Tr}\rho - 1)$  in the above equation implements the fixed-trace condition; that is, all eigenvalues  $\{\mu_i\}$  of the density matrix  $\rho$  add up to 1. The Heaviside theta function  $\Theta(\rho)$  ensures that the density matrix is positive definite. The corresponding random matrix has the construction [3,46]

$$\rho = \frac{(\mathbb{1}_n + U)AA^\dagger(\mathbb{1}_n + U^\dagger)}{\text{Tr}[(\mathbb{1}_n + U)AA^\dagger(\mathbb{1}_n + U^\dagger)]}, \tag{3}$$

where  $A$  is an  $(n \times m)$ -dimensional complex Ginibre matrix with the associated probability density,

$$P_A(A) \propto \exp(-\text{Tr}AA^\dagger). \tag{4}$$

Further,  $U$  is a unitary matrix from the weighted measure described above. Details of the above construction and how it leads to the BH distribution are provided in Appendix A.

We consider the eigendecomposition

$$\rho = \mathcal{U}^\dagger \mathcal{M} \mathcal{U} \tag{5}$$

of the reduced density matrix defined in Eq. (1) or, equivalently, in Eq. (3). From the structure of the probability density of  $\rho$ , it follows that the dependence on eigenvalues and eigenvectors factorizes. The diagonal matrix  $\mathcal{M}$  consists of the eigenvalues  $\{\mu_i\}$  whose joint probability density is given by [4,8]

$$P_{\text{BH}}^{(F)}(\{\mu_i\}) \propto \prod_{j>k} \frac{(\mu_j - \mu_k)^2}{\mu_j + \mu_k} \delta\left(\sum_{s=1}^n \mu_s - 1\right) \prod_{l=1}^n \mu_l^\alpha \Theta(\mu_l). \tag{6}$$

The superscript  $(F)$  signifies the fixed-trace condition. The  $n$ -dimensional random unitary matrix  $\mathcal{U}$  consists of the eigenvectors corresponding to the above eigenvalues and belongs to the coset space  $U(n)/U^n(1)$ , which fixes the arbitrariness of the eigenvectors associated with phase factors.

In the random-matrix-theory terminology, the joint probability density in Eq. (6) defines the fixed (unit) trace BH ensemble. We should remark that the corresponding unrestricted-trace variant is obtained using the construction  $(\mathbb{1}_n + U)AA^\dagger(\mathbb{1}_n + U^\dagger)$  and has the corresponding joint

probability density of eigenvalues  $\{\lambda_i\}$  given by

$$P_{\text{BH}}(\{\lambda_i\}) \propto \prod_{j>k} \frac{(\lambda_j - \lambda_k)^2}{\lambda_j + \lambda_k} \prod_{l=1}^n \lambda_l^\alpha e^{-\lambda_l} \Theta(\lambda_l). \quad (7)$$

The relation between the above probability density and that of another very important random matrix ensemble, namely, the Cauchy two-matrix model, was established in Ref. [51].

### III. ANALYTICAL RESULTS

We aim to focus on multiple aspects of the results obtained from the coupled-kicked-top simulations by varying the stochasticity and coupling parameters of the system. To begin with, we examine the behavior of bipartite pure states generated in the simulation. Next, we investigate the eigenvalue and eigenvector statistics of the reduced states which are obtained using the procedure laid out in the preceding section. These are expected to belong to the BH ensemble. Finally, we study the average entropies and the local fluctuation properties associated with the empirical spectra.

In the following, we compile the necessary analytical results which will be needed in subsequent sections to analyze the simulation results, as mentioned above. These include new closed-form expressions for the spectral density and arbitrary moments of the fixed-trace BH ensemble and hence of the BH-distributed random density matrices.

#### A. Matrix-element distribution of a random pure state

We want to examine how close the pure states generated in the coupled-kicked-top simulation are to the random pure state generated with the aid of the Haar measure. To that end, we compare the distribution of the matrix elements of the bipartite coupled-kicked-top density matrix in Sec. IV with those of the  $(n \times m)$ -dimensional normalized Ginibre matrix  $\mathcal{A} = A/\sqrt{\text{Tr}AA^\dagger}$ . The  $2nm$ -dimensional vector constructed out of the real and imaginary components of matrix elements of  $\mathcal{A}$  is a uniform random vector on a  $(2nm - 1)$ -dimensional unit sphere. It can be shown that the marginal probability density of the square modulus  $R_{jk} = |\mathcal{A}_{jk}|^2$  for all  $i, j$  is given by  $u(nm, R_{jk})$  [83,84,123], where

$$u(l, R) = \begin{cases} (l-1)(1-R)^{l-2} & \text{for } 0 < R \leq 1, \\ 0 & \text{otherwise.} \end{cases} \quad (8)$$

Another way to obtain this result is based on the observation that the random pure state  $|\psi\rangle$  is obtained by operating a Haar-distributed  $nm$ -dimensional unitary matrix on an arbitrary  $nm$ -dimensional nonzero normalized complex vector. Instead of using  $R_{jk}$  directly, we consider the related quantity  $S_{jk} = \ln(nmR_{jk})$ , for which the probability density function is  $v(nm, S_{jk})$ , given by

$$v(l, S) = \begin{cases} \frac{(l-1)}{l} e^S (1 - \frac{e^S}{l})^{l-2} & \text{for } -\infty < S \leq \ln l, \\ 0 & \text{otherwise.} \end{cases} \quad (9)$$

The logarithm helps in resolving the behavior of the distribution better in the vicinity of origin, and the scaling with  $l$  leads

to the  $l$ -independent result in the high-dimension ( $l \rightarrow \infty$ ) limit.

#### B. Eigenvector and eigenvalue distributions of reduced state

The probability density function of the square modulus of each matrix element of the  $n$ -dimensional unitary matrix  $\mathcal{U}$  is given by  $u(n, |\mathcal{U}_{jk}|^2)$  [83,84,123], which is defined in Eq. (8). Therefore,  $\ln(n|\mathcal{U}_{jk}|^2)$  is distributed as in Eq. (9) with  $l = n$ . This result will be used in Sec. IV to compare the corresponding distribution of the elements of eigenvectors of the reduced state generated using the coupled-kicked-top system.

Next, we focus on the spectral density (marginal eigenvalue density) of the reduced density matrix defined in Eq. (1). The spectral density captures the behavior of a generic eigenvalue of the ensemble and is useful in calculating other observables which are linear statistic on the eigenvalues. The spectral density of the unrestricted-trace BH ensemble, as in Eq. (7), was derived in Ref. [51] in terms of an integral over the product of two Meijer  $G$  functions. In Ref. [50], it was given as a finite double sum with a Pfaffian term. We provide here a new finite-sum expression for the spectral density in terms of the Meijer  $G$  function.

We demonstrate in Appendix B that the spectral density of the unrestricted-trace BH ensemble can be written as

$$p(\lambda) = \frac{1}{2n} [F_\alpha(\lambda) + F_{\alpha+1}(\lambda)], \quad (10)$$

where

$$F_q(\lambda) = \sum_{k=0}^{n-1} C_{k,q} \lambda^{k+2\alpha+1} \times G_{3,4}^{2,2} \left( \begin{matrix} -2\alpha - k - 1, -n - 2\alpha - 1; n \\ 0, -q; -2\alpha - 1, -2\alpha - 2 - k \end{matrix} \middle| \lambda \right), \quad (11)$$

with

$$C_{k,q} = \frac{(-1)^k (k + 2\alpha + 2)_n}{\Gamma(n - k) \Gamma(k + 2\alpha + 2 - q) k!}. \quad (12)$$

Here,  $(a)_b = \Gamma(a + b)/\Gamma(a)$  denotes the Pochhammer symbol. The spectral density can be used to calculate an arbitrary order moment of the eigenvalues. As is also shown in Appendix B, we have

$$\langle \lambda^\eta \rangle = \int_0^\infty \lambda^\eta p(\lambda) d\lambda = \sum_{k=0}^{n-1} D_{k,\eta}, \quad (13)$$

where

$$D_{k,\eta} = \frac{(-1)^{k+1} (\eta + 2k + 2\alpha + 2)}{2n\eta\Gamma(n-k)k!} \times \frac{(-\eta - k)_n (k + \alpha + 2)_{\eta-1} (k + 2\alpha + 2)_n}{(\eta + k + 2\alpha + 2)_n}. \quad (14)$$

It should be noted that  $(-\eta - k)_n$  is the same as  $(-1)^\eta (\eta + k + 1 - n)_n$ . Moreover, for  $\eta \rightarrow 0$ ,  $\langle \lambda^\eta \rangle = 1$  is obtained as a limit.

The spectral density of the fixed-trace BH ensemble and therefore of the BH-distributed random density matrices can

be obtained from the above result via a Laplace inversion [50],

$$p^{(F)}(\mu) = \Gamma[n(n + 2\alpha + 1)/2] \times \mathcal{L}^{-1}\{s^{1-n(n+2\alpha+1)/2} p(s\mu)\}(t)|_{t=1}. \quad (15)$$

We use the Laplace inversion formula provided in Ref. [124] for the Meijer  $G$  function to obtain the desired expression as

$$p^{(F)}(\mu) = \frac{1}{2n} [G_\alpha(\mu) + G_{\alpha+1}(\mu)], \quad (16)$$

where

$$G_q(\mu) = \Gamma[n(n + 2\alpha + 1)/2] \sum_{k=0}^{n-1} C_{k,q} \mu^{k+2\alpha+1} \times G_{4,4}^{2,2} \left( \begin{matrix} -2\alpha - k - 1, -n - 2\alpha - 1; n, n(n + 2\alpha + 1)/2 - 2\alpha - k - 2 \\ 0, -q; -2\alpha - 1, -2\alpha - 2 - k \end{matrix} \middle| \mu \right). \quad (17)$$

Finally, from Eq. (15), it can be readily shown that the  $\eta$ th moment of the fixed-trace BH ensemble is related to that of the unrestricted-trace variant as

$$\langle \mu^\eta \rangle = \frac{\Gamma[n(n + 2\alpha + 1)/2]}{\Gamma[\eta + n(n + 2\alpha + 1)/2]} \langle \lambda^\eta \rangle. \quad (18)$$

We will compare the expression for the BH spectral density appearing in Eq. (16) with those obtained from coupled-kicked-top simulations in Sec. IV.

### C. Average entropies

Entropy measures like von Neumann entropy and purity help us conclude how close a random density matrix is to being pure or maximally mixed. The von Neumann entropy is given by

$$S = -\text{Tr}(\rho \ln \rho) = -\sum_{i=1}^n \mu_i \ln \mu_i. \quad (19)$$

For a pure state, the von Neumann entropy is zero, and in the maximally mixed case it acquires the value  $\ln n$ . The purity is given by

$$S_p = \text{Tr}(\rho^2) = \sum_{i=1}^n \mu_i^2. \quad (20)$$

For a pure state the purity is 1, whereas the maximally mixed case corresponds to a value of  $1/n$ . The average purity can be obtained as  $\langle S_p \rangle = n \langle \mu^2 \rangle$ , and hence, the corresponding result can be read from Eq. (18) for  $\eta = 2$ . Alternative exact results for the average entropies were calculated in Ref. [50] as finite sums, and additionally, their compact expressions were also conjectured. These conjectures were proved very recently in Ref. [80] by explicitly evaluating sums similar to that in Eq. (13). The average von Neumann entropy turns out to be

$$\langle S \rangle = \psi(mn - n^2/2 + 1) - \psi(m + 1/2) = \begin{cases} \sum_{j=1}^{mn-n^2/2} j^{-1} - \sum_{j=1}^m (j - 1/2)^{-1} + 2 \ln 2, & n \text{ even,} \\ \sum_{j=m+1}^{mn-(n^2-1)/2} (j - 1/2)^{-1}, & n \text{ odd,} \end{cases} \quad (21)$$

and the average purity is given by

$$\langle S_p \rangle = \frac{2m(2m + n) - (n^2 - 1)}{2m(2mn - n^2 + 2)}. \quad (22)$$

Here,  $\psi(y) = [1/\Gamma(y)] \int_0^\infty e^{-u} u^{y-1} \ln u \, du$  is the digamma function.

### D. Local fluctuation properties

It is well acknowledged that local fluctuation properties of the spectra of quantum chaotic systems coincide with those of random matrices [35,125,126]. The quantum kicked top whose classical limit exhibits chaotic behavior [6] has already been employed to study the statistical properties of the eigenvalues from the HS ensemble. It was found that in the limit of high-dimensional matrices, these properties match RMT predictions [14,28]. This motivates us to study the local fluctuation properties of the BH eigenvalues by considering the ratio of eigenvalue spacings as the measure. In comparison to the nearest-neighbor spacing distribution, it is advantageous to consider the ratio of nearest-neighbor spacings as unfolding is not required in this case. We show in later sections that in the strongly chaotic regime, fluctuation properties of high-dimensional square density matrices belonging to the BH ensemble approach the Wigner-surmise-like result for GUE random matrices [109,110].

To touch upon these results, let us say we have an ordered set of energy levels  $e_1 < e_2 < e_3 \dots < e_j < e_{j+1} \dots$ . The ratio of consecutive eigenvalue spacings is then given as  $r_j = (e_{j+2} - e_{j+1}) / (e_{j+1} - e_j)$ . The Wigner-surmise-like result for the ratio of consecutive spacings for GUE is given by [109,110,122]

$$P_r(r) = \frac{81\sqrt{3}}{4\pi} \frac{(r + r^2)^2}{(1 + r + r^2)^4}. \quad (23)$$

This is an exact result based on a  $3 \times 3$  random matrix model.

## IV. COUPLED KICKED TOP

The Hamiltonian for the coupled kicked top is defined by [87,97,98]

$$H = H_1 \otimes \mathbb{1}_m + \mathbb{1}_n \otimes H_2 + H_{12}. \quad (24)$$



Here,

$$H_s = \frac{\pi}{2} J_{y_s} + \frac{\kappa_s}{2j_s} J_{z_s}^2 \sum_{\nu=-\infty}^{\infty} \delta(t - \nu), \quad s = 1, 2, \quad (25)$$

represent the Hamiltonians for the individual tops, and

$$H_{12} = \frac{\epsilon}{\sqrt{j_1 j_2}} (J_{z_1} \otimes J_{z_2}) \sum_{\nu=-\infty}^{\infty} \delta(t - \nu) \quad (26)$$

gives the interaction term. The first term in  $H_s$  signifies the free precession of the  $s$ th top around the  $y$  axis with an angular frequency  $\pi/2$ , and the second term contains the periodic  $\delta$ -function kicks. The stochasticity parameters  $\kappa_1$  and  $\kappa_2$  measure the strength of the kicks for the two tops and decide their individual chaotic behaviors in the uncoupled case.  $j_s$  is the quantum number corresponding to the operator  $J_s^2 = J_{x_s}^2 + J_{y_s}^2 + J_{z_s}^2$ . The Hamiltonians  $H_1$  and  $H_2$  are associated with  $(n = 2j_1 + 1)$ - and  $(m = 2j_2 + 1)$ -dimensional Hilbert spaces  $\mathcal{H}^{(n)}$  and  $\mathcal{H}^{(m)}$ , respectively. The Hamiltonian for the coupled kicked tops corresponds to an  $(nm)$ -dimensional Hilbert space  $\mathcal{H}^{(nm)} = \mathcal{H}^{(n)} \otimes \mathcal{H}^{(m)}$ . The parameter  $\epsilon$  takes care of the coupling between the two tops.

The unitary Floquet operator corresponding to the coupled Hamiltonian in Eq. (24), which time evolves a state vector from immediately after one kick to immediately after the next, is given by

$$\mathcal{F} = \mathcal{F}_{12}(\mathcal{F}_1 \otimes \mathcal{F}_2), \quad (27)$$

where

$$\mathcal{F}_s = \exp\left(-\frac{\iota \kappa_s}{2j_s} J_{z_s}^2\right) \exp\left(-\frac{\iota \pi}{2} J_{y_s}\right), \quad s = 1, 2, \quad (28)$$

$$\mathcal{F}_{12} = \exp\left(-\frac{\iota \epsilon}{\sqrt{j_1 j_2}} J_{z_1} \otimes J_{z_2}\right), \quad (29)$$

with  $\iota = \sqrt{-1}$  being the imaginary-number unit. The product form of exponentials in writing the Floquet operator follows due to the fact that the operators for the two independent tops commute and that between the  $\delta$ -function kicks only free-precession parts of the Hamiltonian survive, while at the instants of the kicks they are ineffective [6].

Before we proceed further, it would be helpful to summarize the behavior exhibited by the kicked-top system with the choice of the stochasticity and coupling parameters, as established in earlier studies. The classical and quantum aspects of a single kicked top were studied in great detail in Refs. [7,86,87,97]. The classical limit is obtained in  $j \rightarrow \infty$ , which plays the role of  $1/\hbar$ . The resulting classical map exhibits a rich variety of behaviors in the associated phase space as the stochasticity parameter  $\kappa$  is varied. The system is completely integrable for  $\kappa = 0$ . As  $\kappa$  is gradually increased, stochastic regions begin to emerge for  $\kappa \approx 2$ . Around  $\kappa = 3$ , the phase space exhibits a mixed behavior with many stochastic points and periodic orbits coexisting. For  $\kappa = 6$ , the phase space is dominantly chaotic with only a few very tiny regular islands of stability. In the corresponding quantum variant, the chaos manifests in the fluctuation properties of the eigenphases of the Floquet operator and is found to be consistent with random matrix theory [6,7]. For the coupled

kicked top, the overall behavior is decided by the stochasticity parameters  $\kappa_1, \kappa_2$  associated with the two tops and the coupling parameter  $\epsilon$  [87,97]. For relatively weak couplings ( $\epsilon \lesssim 10^{-2}$ ), the degree of chaos in the system is determined prominently by the behavior of the individual tops, i.e., the corresponding  $\kappa_1, \kappa_2$  values. For such weak couplings, it has been found that the eigenvalue density of the reduced density matrix obtained from the coupled kicked top, and hence the bipartite entanglement behavior, agrees with the random matrix Hilbert-Schmidt ensemble results only for large values of  $j_1, j_2$  ( $\gtrsim 100$ ) [97,107]. On the other hand, if the coupling constant is assigned sufficiently large values ( $\sim 1$ ), the random matrix behavior is achieved in the Schmidt eigenvalues for rather small values of  $j_1, j_2$  ( $\sim 10$ ) [34,98,104]. This can be attributed to the significant amount of interaction between the two tops, which plays a crucial role in deciding the overall behavior of the system. Since we are interested in comparing finite-dimension analytical results with those obtained from the coupled-kicked-top simulation, here also, our focus is on small dimensions and a significant amount of coupling. It should be noted that in such a setup, one does not strictly have the classical correspondence. However, for the sake of simplicity, we still refer to the individual tops as integrable, mixed type, or chaotic based on the values of the corresponding stochasticity parameters  $\kappa_1$  and  $\kappa_2$ .

### Generating the density matrices

In this section, we describe the procedure for generating the bipartite pure density matrix corresponding to the coupled-kicked-top system and also the reduced density matrix as per the prescription in Eq. (1).

The initial states for the individual tops are chosen to be directed angular momentum states [6]. In the  $|j_s, m_s\rangle$  basis, they are given by  $\langle j_s, m_s | \theta_s, \phi_s \rangle = (1 + |\gamma_s|^2)^{-j_s} \gamma_s^{j_s - m_s} \sqrt{\binom{2j_s}{j_s + m_s}}$ , with  $\gamma_s \equiv \exp(\iota \phi_s) \tan(\theta_s/2)$ . We define  $n$ - (for  $s = 1$ ) and  $m$ - (for  $s = 2$ ) dimensional vectors, given by [87,96–98,104]

$$\chi_s = [\langle j_s, m_s | \theta_s, \phi_s \rangle]_{m_s = -j_s \dots j_s} \quad (30)$$

for use in creating the initial states of the coupled kicked top. The initial  $(n \times m)$ -dimensional matrix representation for the state of the coupled system is given by the direct product of the initial states of the two tops, viz.,  $\psi(0) = \chi_1 \otimes \chi_2^T$ . This corresponds to the product state  $|\theta_1, \phi_1\rangle \otimes |\theta_2, \phi_2\rangle$ .

Given a state  $|\psi(\nu)\rangle$ , the next state  $|\psi(\nu + 1)\rangle$  can be created by operating the time-evolution operator on it,

$$|\psi(\nu + 1)\rangle = \mathcal{F}|\psi(\nu)\rangle = \mathcal{F}_{12}(\mathcal{F}_1 \otimes \mathcal{F}_2)|\psi(\nu)\rangle. \quad (31)$$

This iteration scheme in matrix representation is given by

$$\psi(\nu + 1) = \mathcal{F}_{12} \circ [\mathcal{F}_1 \psi(\nu) \mathcal{F}_2^T]. \quad (32)$$

Here,  $\circ$  represents the Hadamard product, and  $T$  gives the transpose.  $\mathcal{F}_{12}$  is an  $(n \times m)$ -dimensional matrix represented by

$$\mathcal{F}_{12} = \left[ \exp\left(-\iota \frac{\epsilon}{\sqrt{j_1 j_2}} ab\right) \right]_{\substack{a=-j_1 \dots +j_1 \\ b=-j_2 \dots +j_2}}. \quad (33)$$

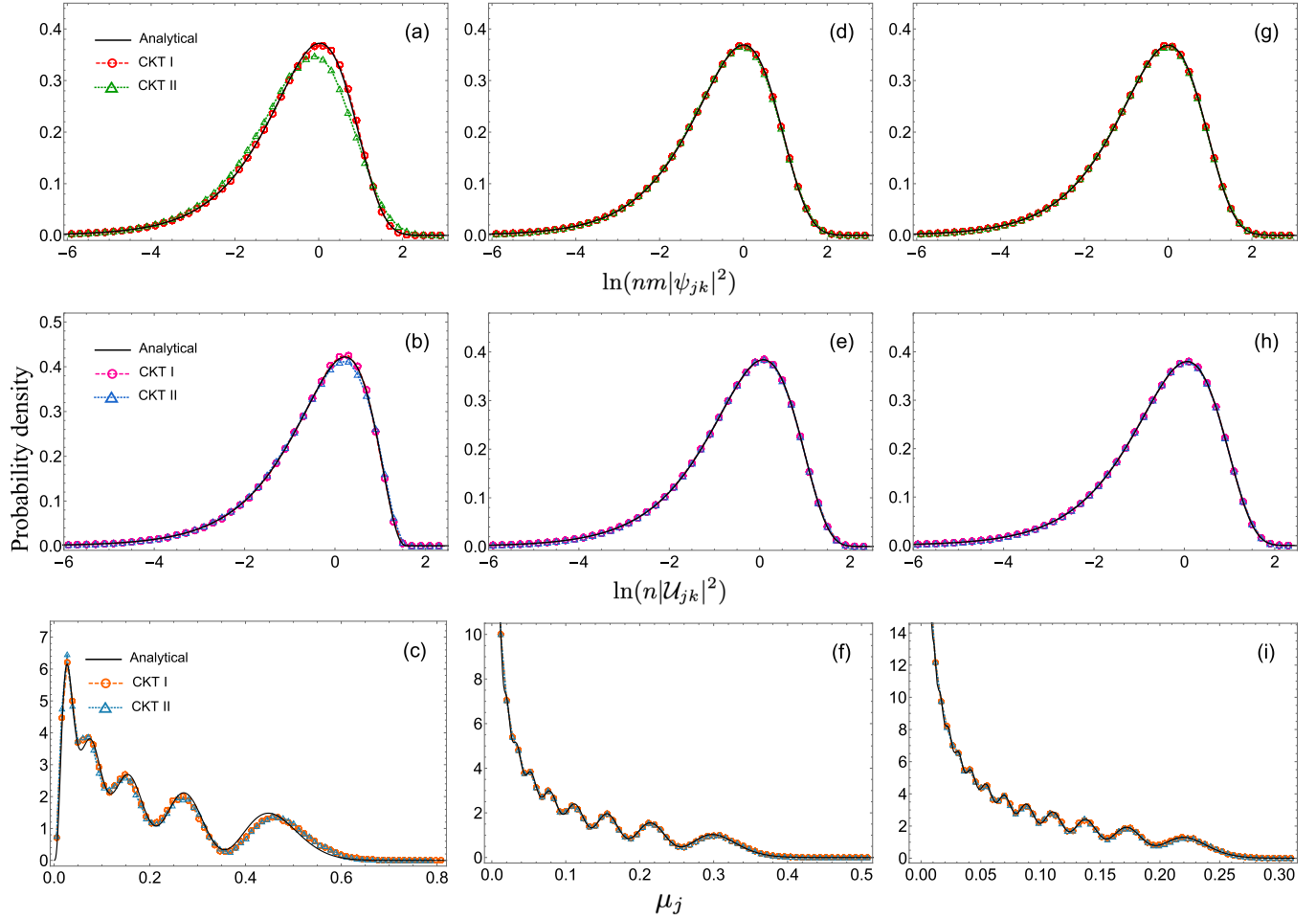


FIG. 1. Distributions of matrix elements of the bipartite pure state (top row) and eigenvector elements (middle row) and eigenvalues (bottom row) of the reduced state. The symbols depict results based on coupled-kicked-top (CKT) simulations performed using two different initial conditions:  $(\theta_1, \phi_1; \theta_2, \phi_2) = (0.83, 0.65; 0.80, 0.60)$  and  $(0.53, 0.31; 0.24, 0.45)$ , which have been indicated as CKT I and CKT II. The solid lines depict the appropriate random-matrix-theory-based analytical results. The parameters chosen for simulations are  $(\kappa_1, \kappa_2, \epsilon) = (7, 8, 1)$ . This corresponds to highly chaotic phase space for the two individual tops. The parameter  $\epsilon$  in the present case provides a good amount of coupling between the tops and plays a crucial role in deciding the overall behavior. The dimensions increase in the plots columnwise from left to right as  $(n, m) = (5, 9), (13, 13),$  and  $(17, 19)$ .

$\mathcal{F}_1$  and  $\mathcal{F}_2$  are, respectively,  $(n \times n)$ - and  $(m \times m)$ -dimensional matrices given by

$$\mathcal{F}_s = \left[ \exp \left( -i \frac{k_s}{2j_s} a^2 \right) d_{a,b}^{(j_s)}(\pi/2) \right]_{a,b=-j_s, \dots, +j_s}, \quad (34)$$

where  $d_{a,b}^{(j_s)}$  is the Wigner (small  $d$ ) matrix. An ensemble is created by applying the iteration scheme (32) many times and considering  $\psi(\nu)$  separated by a certain number of  $\nu$  values. Moreover, the transient states generated during initial iterations are not considered for analysis [87,96–98,104]. We use the  $(n \times m)$ -dimensional matrix representation  $\psi$  of the bipartite pure state for comparison with the normalized Ginibre matrix  $\mathcal{A} = A/\sqrt{\text{Tr}AA^\dagger}$ , as described in Sec. III A.

To generate reduced random density matrices according to Eq. (1), we require unitary matrices from the set equipped with the measure  $|\det(\mathbb{1}_n + U)|^{2(m-n)} d\mu(U)$ . It reduces to the Haar measure for  $m = n$ , and therefore, in this case these matrices  $U$  may be taken from the circular unitary ensemble of random matrices. For the general case ( $m \neq n$ ), we

adopt the following strategy. The unitarily invariant nature of  $|\det(\mathbb{1}_n + U)|^{2(m-n)} d\mu(U)$  leads to the joint probability density of the eigenangles  $\{\xi_i\}$  of  $U$  as

$$P_\xi(\{\xi_i\}) \propto \prod_{j>k} \sin^2 \left( \frac{\xi_j - \xi_k}{2} \right) \prod_{l=1}^n (1 + \cos \xi_l)^{m-n}. \quad (35)$$

We generate these eigenangles using the log-gas approach [35,36,127]. The  $U$  matrices are then obtained by conjugating  $\text{diag}(e^{i\xi_1}, \dots, e^{i\xi_n})$  with unitary matrices  $V$  from the Haar measure, i.e.,  $U = V^\dagger \text{diag}(e^{i\xi_1}, \dots, e^{i\xi_n})V$ . Eventually, these are used to create the desired superposition,

$$\vartheta(\nu) = (\mathbb{1}_n + U)\psi(\nu), \quad (36)$$

where  $\psi(\nu)$  is as in Eq. (32). The reduced density matrix of dimension  $n \times n$  is constructed thereafter as

$$\rho = \frac{\vartheta\vartheta^\dagger}{\text{Tr}(\vartheta\vartheta^\dagger)}. \quad (37)$$

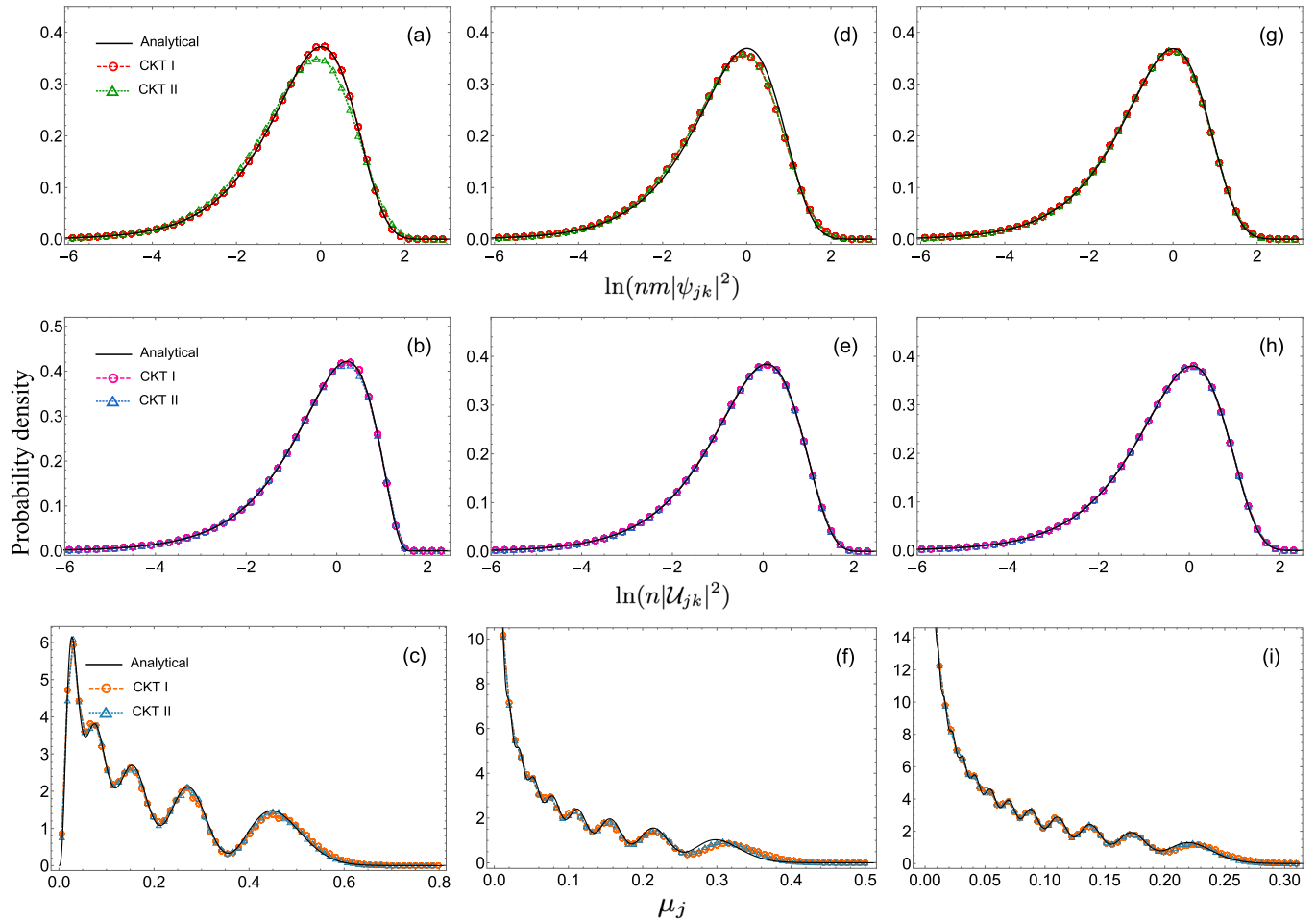


FIG. 2. Plots as in Fig. 1, except for the coupled-kicked-top parameters, which are set to  $(\kappa_1, \kappa_2, \epsilon) = (0.5, 8, 1)$  in this case, which corresponds to the first top being almost integrable and the second top being highly chaotic. The coupling between the two tops remains significant, as in Fig. 1.

These density matrices are expected to be from the BH measure when the parameters of the coupled kicked tops are adequately chosen. Like for Eq. (5), we consider the eigendecomposition of the above  $\rho$  and compare the resulting eigenvectors and eigenvalues with the analytical results of Sec. III B.

At this point, it would be worth discussing the feasibility of generation of the Bures-Hall state and its generalizations in experiments using quantum circuits. It is well established that generation of random pure states and random unitary operators is exponentially hard in these circuits. However, methods of generating pseudorandom states and pseudorandom unitary operators are now known which can be efficiently used in quantum communication and information processing protocols [128]. One such approach which has been very fruitful in recent years is the so-called quantum  $t$  design [129–133]. Such pseudorandom states or unitary operators can mimic properties of the probability distribution over the Haar measure for polynomials of degree up to  $t$ . In other words, these  $t$  designs simulate up to  $t$ th-order statistical moments of the original ensemble. Therefore, by implementing more sophisticated algorithms in quantum circuits, it might be possible to generate pseudorandom states and unitary operators from nonuniform measures such as the ones discussed above.

## V. COMPARISON OF COUPLED-KICKED-TOP RESULTS WITH RMT

In this section we compare the results of the coupled-kicked-top simulation described in the preceding section with the RMT-based analytical results in Sec. III.

### A. Matrix elements of the bipartite pure state and eigenvectors and eigenvalues of the reduced state

Here, we compare the distribution of matrix elements of the bipartite pure state and the eigenvector and eigenvalues of the reduced state generated in the kicked-top simulation with the analytical results. For the bipartite pure state  $\psi$ , we consider the matrix elements  $\psi_{jk}$  for all  $j, k$  and examine the distribution of  $\ln(nm|\psi_{jk}|^2)$ . This gives the information regarding the behavior of a generic matrix element of  $\psi$ . Likewise, for the reduced state  $\rho$ , we consider the distribution of  $\ln(n|U_{jk}|^2)$ . Finally, the density of eigenvalues of  $\rho$  is also examined. The resulting plots are shown in Figs. 1–5 for various combinations of the stochasticity parameters  $\kappa_1, \kappa_2$  and the coupling parameter  $\epsilon$ . Moreover, for each combination of parameters, two different initial conditions have been considered via the values assigned to  $\theta_s$  and

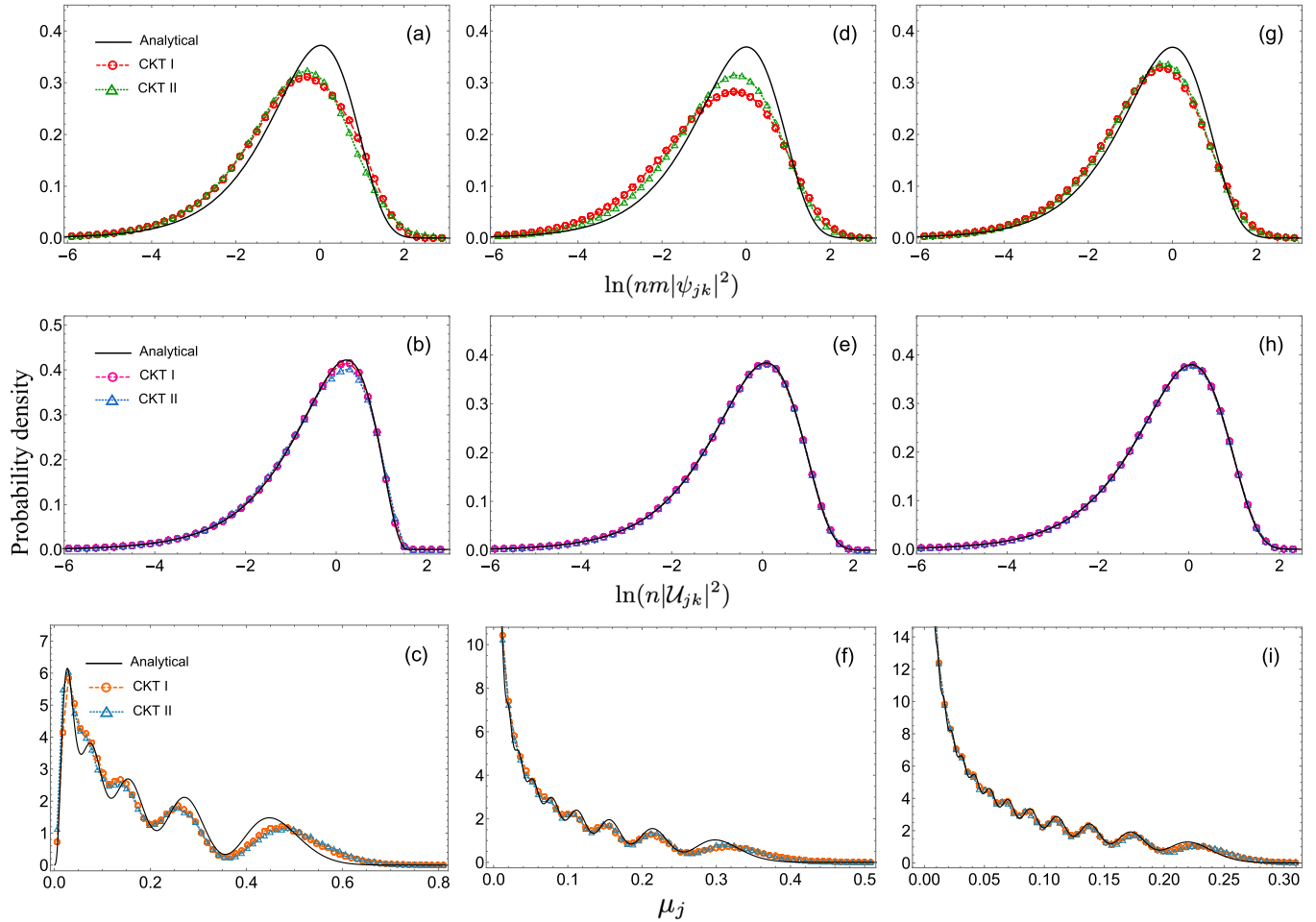


FIG. 3. Plots as in Fig. 1, but with parameters  $(\kappa_1, \kappa_2, \epsilon) = (2.5, 2.5, 1)$ . In this case, the two individual tops exhibit mixed phase-space behavior. The coupling remains significant.

$\phi_s$  in Eq. (30), viz.,  $(\theta_1, \phi_1; \theta_2, \phi_2) = (0.83, 0.65; 0.80, 0.60)$  and  $(0.53, 0.31; 0.24, 0.45)$ .

Figure 1 depicts the plots for parameter choices  $(\kappa_1, \kappa_2, \epsilon) = (7, 8, 1)$ . This combination corresponds to the highly chaotic regime for the individual tops when uncoupled. The coupling constant  $\epsilon$ , which has been assigned a significant value in this case, plays an important role in deciding the overall behavior of the coupled system [97]. For small  $n = 2j_1 + 1$  and  $m = 2j_2 + 1$  values there is some noticeable difference between the kicked-top simulation and analytical results. However, with increasing dimension, as we go from left to right in the plots, the agreement becomes extremely good. In Fig. 2, we keep the values of  $\kappa_2$  and  $\epsilon$  the same as in Fig. 1 but reduce the  $\kappa_1$  value to 0.5, for which the first top exhibits a regular behavior, i.e., when examined without the coupling. In this case also, the empirical distributions are reasonably close to the analytical predictions, especially for higher  $n, m$  values. This can be attributed to the significant amount of interaction between the two tops. A similar phenomenon was observed for the eigenvalues of the HS state generated using coupled kicked tops in Ref. [104]. Next, in Fig. 3, we consider  $(\kappa_1, \kappa_2) = (2.5, 2.5)$ , which gives the mixed phase space for the two tops. The coupling constant  $\epsilon$  is still fixed at 1. We observe that in this case, compared to the last one, the difference between the behavior of matrix elements of the bipartite pure

state and that of uniformly distributed pure states persists even for  $n = 17, m = 19$ . However, the distributions of eigenvector elements of the reduced state and the associated eigenvalues tend to approach the analytical predictions for the BH states, the former with a finer degree. Figure 4 depicts the results for the coupling constant  $\epsilon = 1$  and stochasticity parameters  $\kappa_1 = 0.5$  and  $\kappa_2 = 1$  for which the two tops are individually integrable. In this case, we observe overall large deviations in the empirical distributions for the pure-state matrix elements and the eigenvalues compared to the analytical results. However, the eigenvector elements exhibit behavior close to that of a uniformly distributed vector. Finally, in Fig. 5, we keep  $(\kappa_1, \kappa_2) = (7, 8)$ , corresponding to highly chaotic tops, but reduce the coupling to  $\epsilon = 0.05$ . In this case, the deviation is pronounced in the eigenvalue distribution. On the other hand, the behavior of pure-state matrix elements and eigenvector elements remains close to the analytical results, with the latter having better agreement. In all of the above, we also notice that the empirical curves for the two different initial conditions tend to overlap as the dimensions  $n$  and  $m$  are increased.

Thus, we conclude that all empirical distributions approach the analytical results when the coupling is large enough and the stochasticity parameters are set to high values. Moreover, the agreement improves with increasing  $n$  and  $m$  values, and the effect of the initial condition also gets diminished.



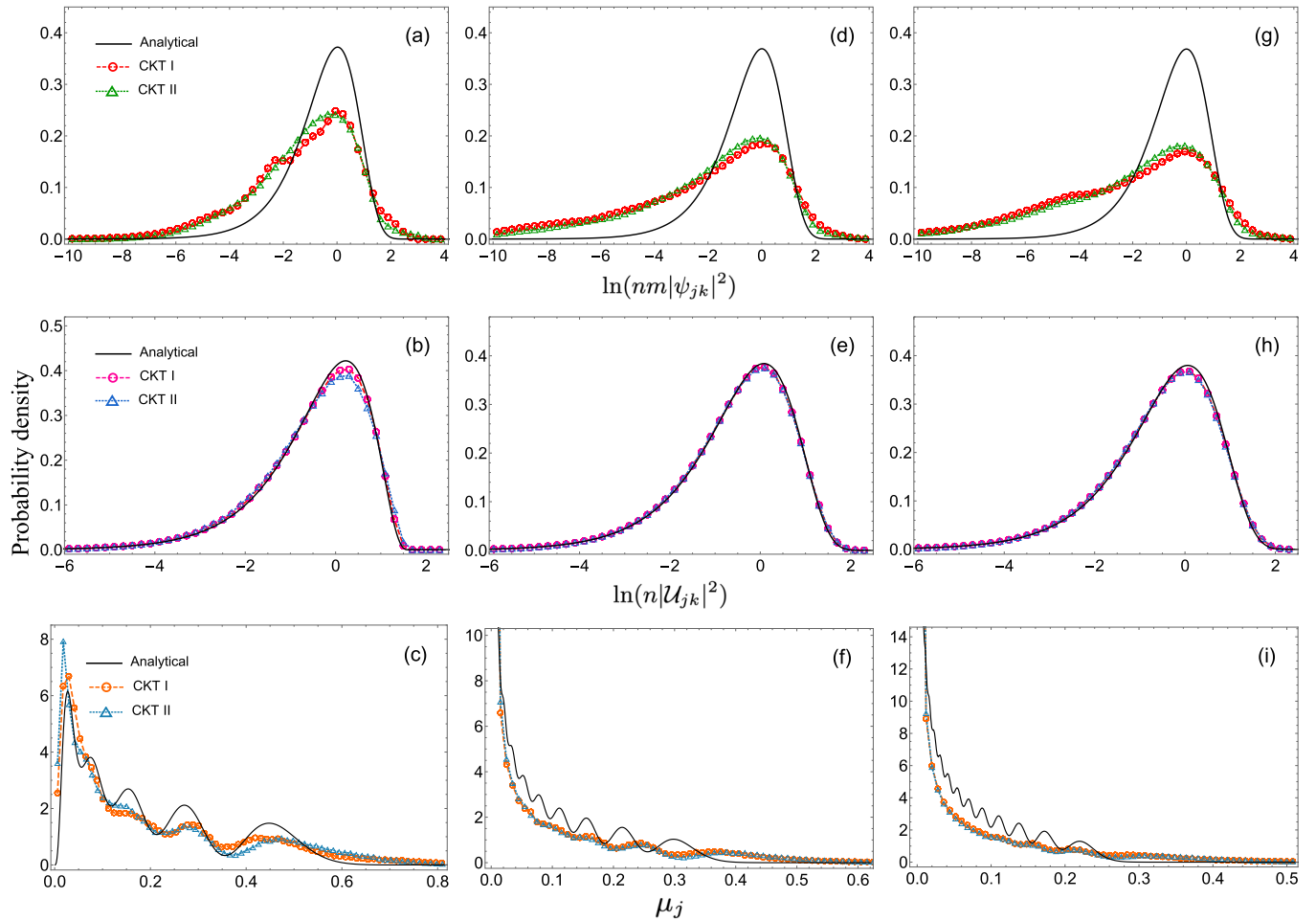


FIG. 4. Plots as in Fig. 1, but with parameters  $(\kappa_1, \kappa_2, \epsilon) = (0.5, 1, 1)$ . Here, the two individual tops exhibit regular behavior. The coupling still remains significant.

### B. Average entropy measures

We now compare the average von Neumann entropy  $\langle S \rangle$  and the average purity  $\langle S_p \rangle$  obtained from the coupled-kicked-top simulation with the BH results given in Sec. III. Figure 6 exhibits the comparison for various combinations of  $\kappa_1, \kappa_2$  with  $\epsilon$  fixed at 1. As expected, the best agreement between the coupled-kicked-top results and RMT is observed for  $(\kappa_1, \kappa_2) = (7, 8)$ . For  $(\kappa_1, \kappa_2) = (0.5, 1)$ , there is a significant deviation from the analytical results.

In Fig. 7, we consider  $\langle S \rangle$  and  $\langle S_p \rangle$  with  $(\kappa_1, \kappa_2) = (7, 8)$  and varying  $\epsilon$ . Very good agreement is seen between the coupled-kicked-top simulation and BH results for  $\epsilon = 0.5$  and 1, with improvements occurring as the dimensions  $n, m$  are increased. For very small couplings, there is significant disagreement between the empirical values and the analytical predictions.

### C. Spectral fluctuation properties of FT Bures-Hall eigenvalues

We now analyze the local fluctuations exhibited by the eigenvalues of the reduced state via the distribution of the ratio of consecutive spacings, as defined in Sec. III D. In Fig. 8, we show the results for  $j_1 = j_2 = 12$ , i.e.,  $n = m = 25$ , and three combinations of the parameters  $\kappa_1, \kappa_2, \epsilon$ . We also display the Wigner-surmise-like result for the ratio

distribution, which is based on  $3 \times 3$  GUE matrices and given in Eq. (23), as a reference in all the plots. We observe that for  $(\kappa_1, \kappa_2, \epsilon) = (7, 8, 1)$ , the ratio distribution from the coupled-kicked-top simulation agrees with the distribution obtained by simulating the BH matrix model given in Eq. (3). For the other two combinations of the parameters, the agreement is not good. We also find that while there is agreement between kicked-top and BH ensemble simulations for the first set of parameters, i.e., when the individual tops are highly chaotic and there is sufficient coupling between them, the empirical ratio distributions are still away from the  $3 \times 3$  GUE result. Therefore, in Fig. 9, we examine the behavior of the ratio distribution by varying the dimensions ( $n = m$ ) but keeping the parameters  $(\kappa_1, \kappa_2, \epsilon)$  fixed at  $(7, 8, 1)$ . We find that, indeed, as the dimensions increase, the empirical ratio distribution approaches the  $3 \times 3$  GUE result, although the convergence is rather slow.

## VI. SUMMARY

In this work, our aim has been to generate Bures-Hall distributed density matrices using the system of coupled kicked tops. Although random matrix models and algorithms to construct density matrices from the Bures-Hall measure have been discussed in the literature, they have not been studied

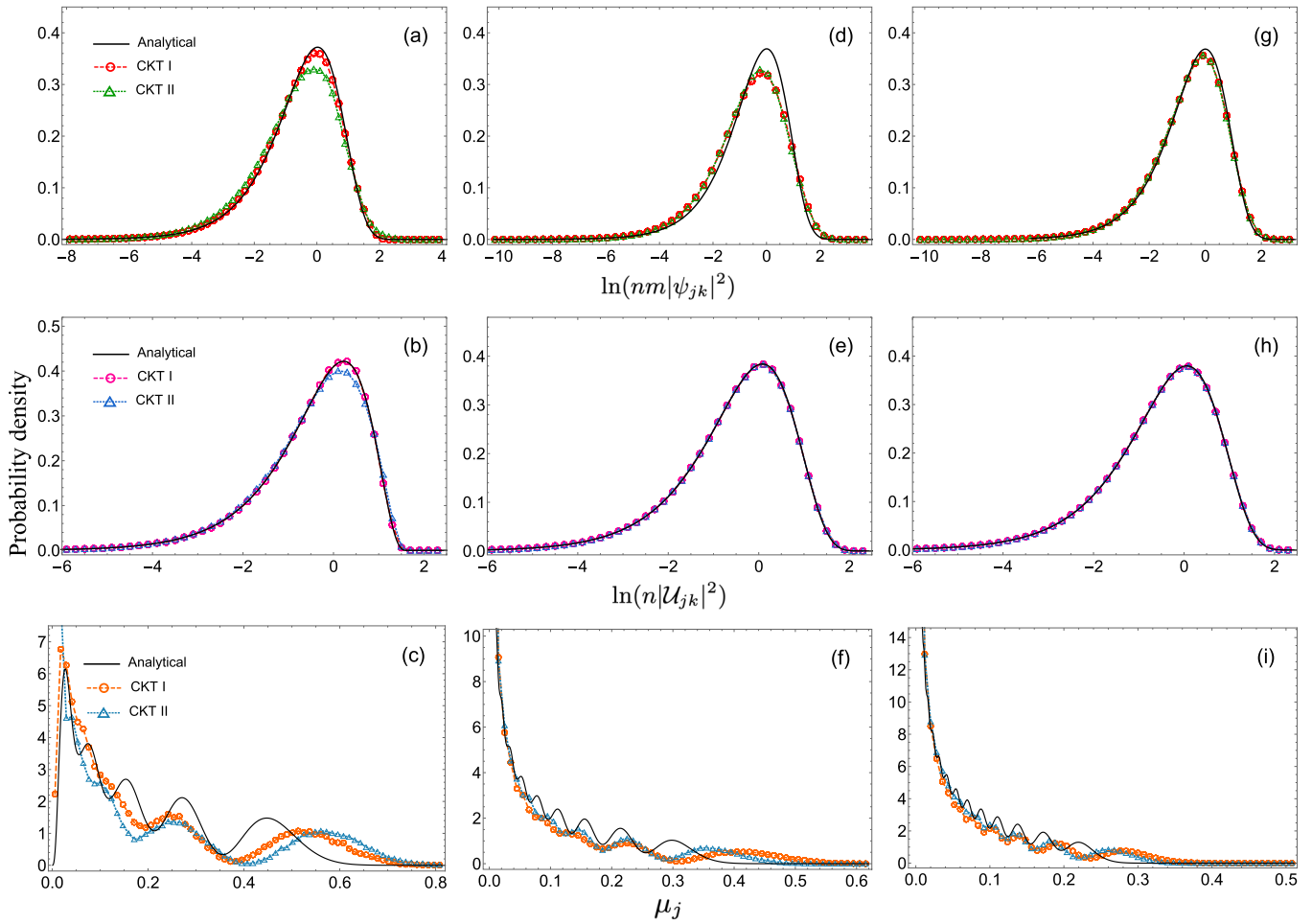


FIG. 5. Plots as in Fig. 1, but with parameters  $(\kappa_1, \kappa_2, \epsilon) = (7, 8, 0.05)$ . The two tops individually again fall in the regime of a high degree of chaos as in Fig. 1; however, the coupling between the two tops has been considerably reduced.

in the context of quantum chaotic systems like the coupled kicked tops. The present work, therefore, fills this gap by studying this ensemble in the light of quantum chaos and complements similar studies done for the Hilbert-Schmidt ensemble.

We have carried out a detailed study of the distributions of the eigenvalues and eigenvectors and also the average entropies with variation in the stochasticity and coupling parameters of the coupled-kicked-top system. Additionally, we have also examined the distribution of the matrix elements of

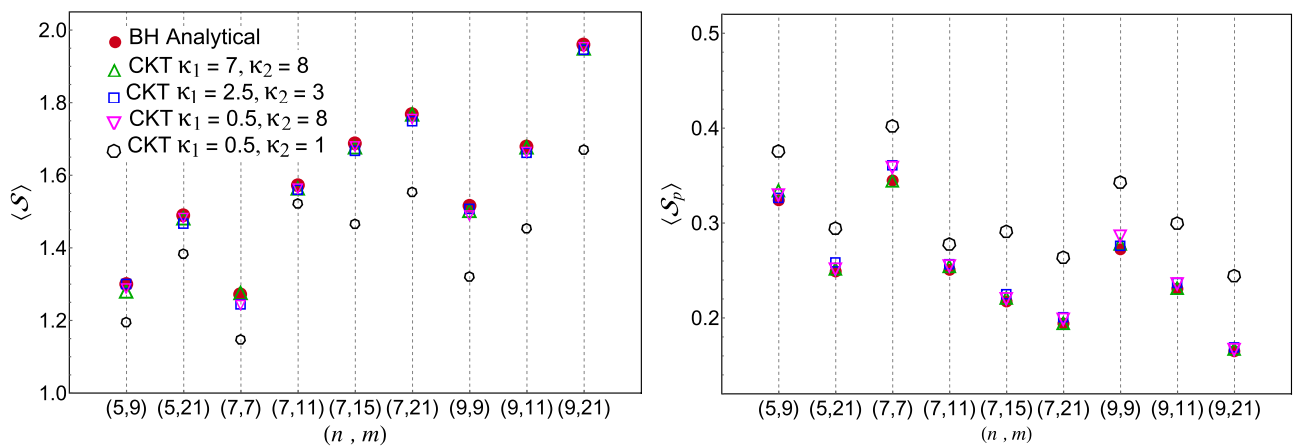


FIG. 6. Average von Neumann entropy  $\langle S \rangle$  and average purity  $\langle S_p \rangle$  as functions of dimensions  $(n, m)$  for various values of  $\kappa_1, \kappa_2$ , and  $\epsilon = 1$ .

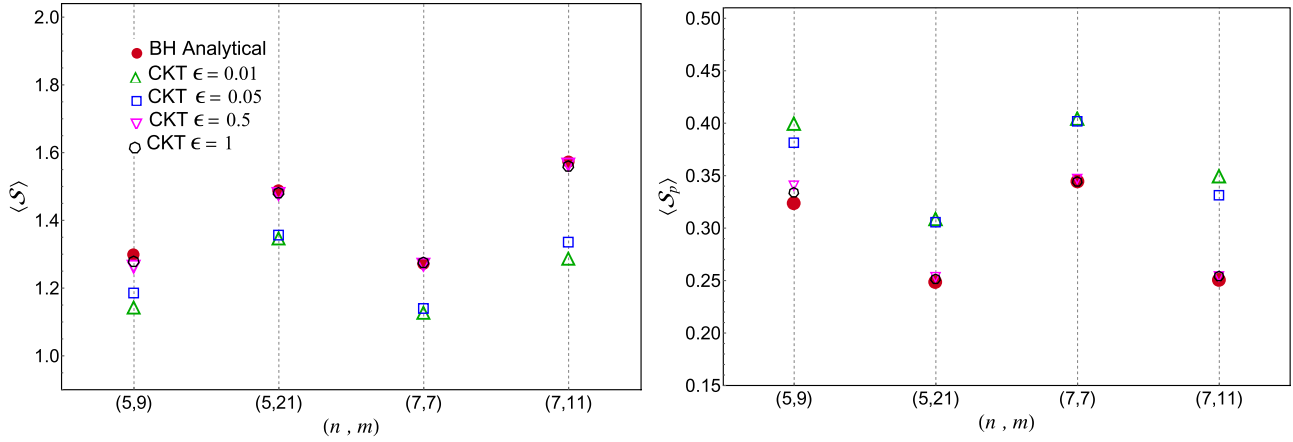


FIG. 7. Average von Neumann entropy  $\langle S \rangle$  and average purity  $\langle S_p \rangle$  as functions of dimensions  $(n, m)$  for fixed  $\kappa_1 = 7, \kappa_2 = 8$  and varying  $\epsilon$ .

the bipartite pure states generated in the kicked top simulation. Like for the Hilbert-Schmidt ensemble, we have found very good agreement with the analytical results in the strongly chaotic regime and when the subsystems representing the two tops have a significant amount of coupling between them. Furthermore, the agreement improves, in general, with increasing dimensionalities. The match reduces notably when the stochasticity parameters for the two tops are small or when the coupling is low between them.

Another line of our investigation regarded the study of spectral fluctuation properties of the eigenvalues of the reduced state using the distribution of the consecutive-spacing ratio. We have found that the results of coupled kicked tops, with adequate parameter values, match those based on the matrix model for the Bures-Hall ensemble. Furthermore, for high-dimensional reduced density matrices, the empirical results for the ratio distribution approach the Wigner-surmise-like result for the Gaussian unitary ensemble of random matrices.

In Ref. [3], the authors introduced a very general class of random states containing an ensemble of non-Hermitian random matrices parameterized by an arbitrary  $l$ -dimensional probability vector  $p = \{p_1, \dots, p_l\}$  and a non-negative integer  $s$ , such that

$$\Omega_{l,s} = (p_1 U_1 + p_2 U_2 + \dots + p_l U_l) G_1 \dots G_s. \quad (38)$$

Here  $U_1, \dots, U_l$  denote  $l$  independent random unitary matrices distributed according to the Haar measure, while  $G_1, \dots, G_s$  are independent complex Ginibre matrices. The random density matrix is then obtained as a normalized Wishart-like matrix,

$$\rho_{l,s} = \frac{\Omega_{l,s} \Omega_{l,s}^\dagger}{\text{Tr}(\Omega_{l,s} \Omega_{l,s}^\dagger)}. \quad (39)$$

For  $l = 2$  and  $s = 1$  the typical Bures ensemble is achieved, while for  $l = 2$  and arbitrary  $s$ , a higher-order Bures ensemble is derived. It will be interesting to explore various statistical properties of these density matrices belonging to more general ensembles and to obtain analytical and numerical insights beyond what is currently known. Furthermore, we would like to explore such generalized ensembles for other symmetry classes of random matrices.

**ACKNOWLEDGMENT**

A.S. acknowledges DST-INSPIRE Government of India, for providing a research fellowship (IF170612).

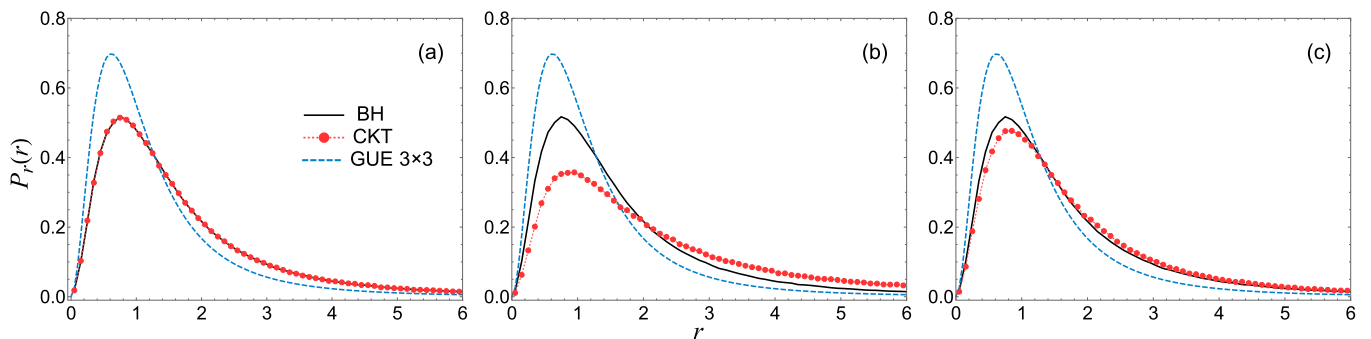


FIG. 8. Ratio distribution for eigenvalues of reduced states obtained in the CKT system with  $n = m = 25$  and three combinations of parameters  $(\kappa_1, \kappa_2, \epsilon)$ : (a)  $(7, 8, 1)$ , (b)  $(0.5, 1, 1)$ , and (c)  $(7, 8, 0.02)$ . Results based on the BH random matrix model are also shown along with the Wigner-surmise-like result ( $\text{GUE} = 3 \times 3$ ).

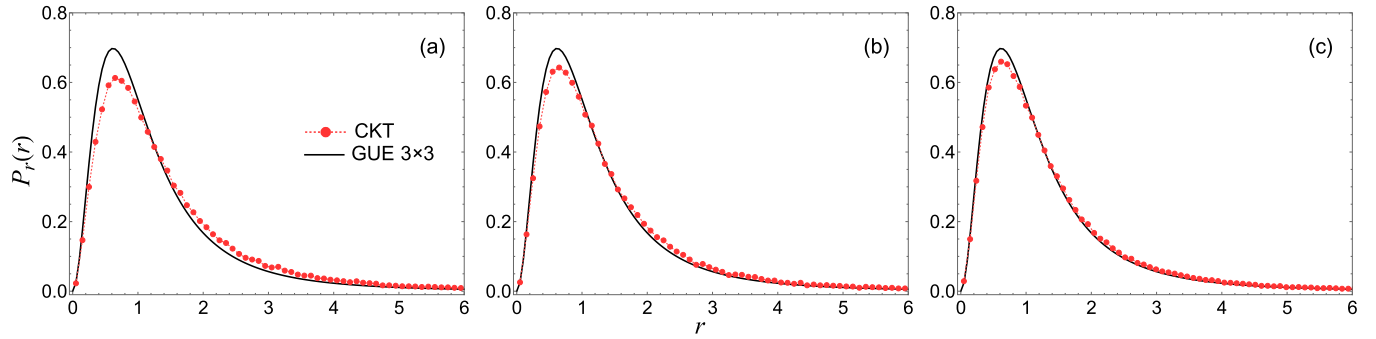


FIG. 9. Ratio distribution for eigenvalues of reduced states obtained in the CKT system for  $(\kappa_1, \kappa_2, \epsilon) = (7, 8, 1)$  with increasing dimensions  $(n, m)$ : (a) (75,75), (b) (151,151), and (c) (251,251). For comparison, the Wigner-surmise-like result (GUE =  $3 \times 3$ ) is also shown.

### APPENDIX A: DERIVATION OF THE WEIGHTED UNITARY MATRICES

In Ref. [46], Osipov *et al.* derived the random matrix model corresponding to the BH-distributed density matrices for the square case, i.e.,  $n = m$ . For this case, one requires Haar-distributed unitary matrices in the construction of density matrices. However, for the general case of  $n \leq m$ , the random unitary matrix  $U$  has to be chosen from the measure  $|\det(\mathbb{1}_n + U)|^{2(m-n)} d\mu(U)$ , which reduces to the Haar measure  $d\mu(U)$  for  $n = m$ . While this was mentioned in some earlier works [50,51], details have not been provided. For the sake of completeness, we outline a derivation below which closely follows that for the square case given in Ref. [46].

It is known that the BH probability density, as given in Eq. (2), can be obtained by the following integral over an  $n$ -dimensional random Hermitian matrix  $H$  and an  $(n \times m)$ -dimensional complex Ginibre matrix  $A$  [46],

$$\mathcal{P}_{\text{BH}}(\rho) \propto \int dA \int dH e^{-\text{Tr}[(\mathbb{1}_n + H^2)AA^\dagger]} \delta\left(\rho - \frac{AA^\dagger}{\text{Tr}AA^\dagger}\right). \quad (\text{A1})$$

Applying a scaling  $A \rightarrow (\mathbb{1}_n + iH)^{-1}A$  leads to the expression

$$\mathcal{P}_{\text{BH}}(\rho) \propto \int \frac{dH}{|\det(\mathbb{1}_n + H^2)|^m} \int dA e^{-\text{Tr}AA^\dagger} \times \delta\left(\rho - \frac{(\mathbb{1}_n + iH)^{-1}AA^\dagger(\mathbb{1}_n - iH)^{-1}}{\text{Tr}[(\mathbb{1}_n + iH)^{-1}AA^\dagger(\mathbb{1}_n - iH)^{-1}]}\right). \quad (\text{A2})$$

Now, Cayley transformation asserts that a unitary matrix  $U$  can be written in terms of a Hermitian matrix  $H$  as  $U = (\mathbb{1}_n - iH)(\mathbb{1}_n + iH)^{-1} = 2(\mathbb{1}_n + iH)^{-1} - \mathbb{1}$ . This gives  $4^n |\det(\mathbb{1}_n + H^2)|^{-1} = |\det(\mathbb{1}_n + U)|^2$ . It is also known that the Haar measure  $d\mu(U)$  is equivalent to the Cauchy-like measure  $dH / [\det(\frac{\mathbb{1}_n + H^2}{2})]^n$  [46]. Therefore, the integral over  $H$  in the above expression may be replaced by an integral over  $U$ , and one gets, after some simplification,

$$\mathcal{P}_{\text{BH}}(\rho) \propto \int d\mu(U) |\det(\mathbb{1}_n + U)|^{2(m-n)} \int dA e^{-\text{Tr}AA^\dagger} \times \delta\left(\rho - \frac{(\mathbb{1}_n + U)AA^\dagger(\mathbb{1}_n + U^\dagger)}{\text{Tr}[(\mathbb{1}_n + U)AA^\dagger(\mathbb{1}_n + U^\dagger)]}\right). \quad (\text{A3})$$

This proves that for general  $m, n$ , the BH-distributed random density matrix  $\rho$  indeed has the construction given in Eq. (3).

### APPENDIX B: DERIVATION OF THE SPECTRAL DENSITY AND ARBITRARY MOMENTS FOR THE UNRESTRICTED-TRACE ENSEMBLE

The spectral density of the unrestricted-trace Bures-Hall ensemble is known as [51]

$$p(\lambda) = \frac{1}{2n} [F_\alpha(\lambda) + F_{\alpha+1}(\lambda)], \quad (\text{B1})$$

where

$$F_q(\lambda) = \int_0^1 dt G_{2,3}^{1,1} \left( \begin{matrix} -n; n+2\alpha+1 \\ 2\alpha+1; 0, q \end{matrix} \middle| t\lambda \right) \times G_{2,3}^{2,1} \left( \begin{matrix} -n-2\alpha-1; n \\ 0, -q; -2\alpha-1 \end{matrix} \middle| t\lambda \right). \quad (\text{B2})$$

In order to compute the above integral, we use the property that the first Meijer  $G$  function inside the integral in Eq. (B2) can be expanded as a finite series [51,52,134],

$$G_{2,3}^{1,1} \left( \begin{matrix} -n; n+2\alpha+1 \\ 2\alpha+1; 0, q \end{matrix} \middle| z \right) = \sum_{k=0}^{n-1} C_{k,q} z^{k+2\alpha+1}, \quad (\text{B3})$$

where

$$C_{k,q} = \frac{(-1)^k (k+2\alpha+2)_n}{\Gamma(n-k)\Gamma(k+2\alpha+2-q)k!}. \quad (\text{B4})$$

Using Eq. (B3) in Eq. (B2), we get

$$F_q(\lambda) = \sum_{k=0}^{n-1} C_{k,q} \lambda^{k+2\alpha+1} \times \int_0^1 t^{k+2\alpha+1} G_{2,3}^{2,1} \left( \begin{matrix} -n-2\alpha-1; n \\ 0, -q; -2\alpha-1 \end{matrix} \middle| t\lambda \right) dt. \quad (\text{B5})$$



This integral can be performed using a result given in Ref. [134], giving us

$$F_q(\lambda) = \sum_{k=0}^{n-1} C_{k,q} \lambda^{k+2\alpha+1} \times G_{3,4}^{2,2} \left( \begin{matrix} -2\alpha - k - 1, -n - 2\alpha - 1; n \\ 0, -q; -2\alpha - 1, -2\alpha - 2 - k \end{matrix} \middle| \lambda \right), \quad (\text{B6})$$

and therefore, Eq. (10) follows.

We also calculate the  $\eta$ th-order moments for the eigenvalues as

$$\langle \lambda^\eta \rangle = \int_0^\infty \lambda^\eta p(\lambda) d\lambda = \frac{1}{2n} \int_0^\infty \lambda^\eta [F_\alpha(\lambda) + F_{\alpha+1}(\lambda)] d\lambda = \frac{1}{2n} [w_\alpha + w_{\alpha+1}]. \quad (\text{B7})$$

The integral  $w_q = \int_0^\infty \lambda^\eta F_q(\lambda) d\lambda$  can be calculated by using the Mellin transform of the Meijer  $G$  function [134],

$$\int_0^\infty dz z^{s-1} G_{p,q}^{m,n} \left( \begin{matrix} a_1, \dots, a_n; a_{n+1}, \dots, a_p \\ b_1, \dots, b_m; b_{m+1}, \dots, b_q \end{matrix} \middle| \zeta z \right) = \frac{\zeta^{-s} \prod_{j=1}^n \Gamma(1 - a_j - s) \prod_{j=1}^m \Gamma(b_j + s)}{\prod_{j=n+1}^p \Gamma(a_j + s) \prod_{j=m+1}^q \Gamma(1 - b_j - s)}. \quad (\text{B8})$$

This gives

$$\begin{aligned} w_q &= \int_0^\infty d\lambda \lambda^\eta F_q(\lambda) \\ &= \sum_{k=0}^{n-1} C_{k,q} \int_0^\infty d\lambda \lambda^{\eta+k+2\alpha+1} G_{3,4}^{2,2} \left( \begin{matrix} -2\alpha - k - 1, -n - 2\alpha - 1; n \\ 0, -q; -2\alpha - 1, -2\alpha - 2 - k \end{matrix} \middle| \lambda \right) \\ &= - \sum_{k=0}^{n-1} C_{k,q} \frac{(-\eta - k)_n \Gamma(\eta + k + 2\alpha + 2 - q)}{\eta(\eta + k + 2\alpha + 2)_n}. \end{aligned} \quad (\text{B9})$$

Now, using this expression in (B7), we obtain Eq. (13) after some simplification.

---

[1] M. A. Nielsen and I. L. Chuang, *Quantum Computation and Quantum Information* (Cambridge University Press, Cambridge, 2000).

[2] M. Paris and J. Rehacek, *Quantum State Estimation* (Springer, Berlin, 2004).

[3] K. Życzkowski, K. A. Penson, I. Nechita, and B. Collins, *J. Math. Phys.* **52**, 062201 (2011).

[4] M. J. W. Hall, *Phys. Lett. A* **242**, 123 (1998).

[5] W. K. Wootters, *Found. Phys.* **20**, 1365 (1990).

[6] F. Haake, *Quantum Signatures of Chaos*, 3rd ed. (Springer, Berlin, 2010).

[7] F. Haake, M. Kuś, and R. Scharf, *Z. Phys. B* **65**, 381 (1987).

[8] K. Życzkowski and H.-J. Sommers, *J. Phys. A* **34**, 7111 (2001).

[9] H.-J. Sommers and K. Życzkowski, *J. Phys. A* **37**, 8457 (2004).

[10] P. Vivo, M. P. Pato, and G. Oshanin, *Phys. Rev. E* **93**, 052106 (2016).

[11] E. Lubkin, *J. Math. Phys.* **19**, 1028 (1978).

[12] S. Lloyd and H. Pagels, *Ann. Phys. (NY)* **188**, 186 (1988).

[13] D. N. Page, *Phys. Rev. Lett.* **71**, 1291 (1993).

[14] Y. Chen, D.-Z. Liu, and D.-S. Zhou, *J. Phys. A* **43**, 315303 (2010).

[15] P. Vivo, *J. Phys. A* **43**, 405206 (2010).

[16] S. Kumar and A. Pandey, *J. Phys. A* **44**, 445301 (2011).

[17] S. Sen, *Phys. Rev. Lett.* **77**, 1 (1996).

[18] K. Życzkowski and H.-J. Sommers, *J. Phys. A* **36**, 10115 (2003).

[19] V. Cappellini, H.-J. Sommers, and K. Życzkowski, *Phys. Rev. A* **74**, 062322 (2006).

[20] O. Giraud, *J. Phys. A* **40**, 2793 (2007).

[21] U. T. Bhosale, S. Tomsovic, and A. Lakshminarayan, *Phys. Rev. A* **85**, 062331 (2012).

[22] P. Facchi, U. Marzolino, G. Parisi, S. Pascazio, and A. Scardicchio, *Phys. Rev. Lett.* **101**, 050502 (2008).

[23] A. De Pasquale, P. Facchi, G. Parisi, S. Pascazio, and A. Scardicchio, *Phys. Rev. A* **81**, 052324 (2010).

[24] C. Nadal, S. N. Majumdar, and M. Vergassola, *Phys. Rev. Lett.* **104**, 110501 (2010).

[25] C. Nadal, S. N. Majumdar, and M. Vergassola, *J. Stat. Phys.* **142**, 403 (2011).

[26] G. Akemann and P. Vivo, *J. Stat. Mech.* (2011) P05020.

- [27] S. N. Majumdar, *The Oxford Handbook of Random Matrix Theory* (Oxford University Press, Oxford, 2010).
- [28] D.-Z. Liu and D.-S. Zhou, *Int. Math. Res. Not.* **2011**, 725 (2011).
- [29] L. Wei, *Phys. Rev. E* **96**, 022106 (2017).
- [30] L. Wei, *Entropy* **21**, 539 (2019).
- [31] S. N. Majumdar, O. Bohigas, and A. Lakshminarayan, *J. Stat. Phys.* **131**, 33 (2008).
- [32] P. J. Forrester and S. Kumar, *J. Phys. A* **52**, 42LT02 (2019).
- [33] S. Adachi, H. Kubotani, and M. Toda, *J. Phys. A* **52**, 405304 (2019).
- [34] S. Kumar, *Phys. Rev. A* **102**, 012405 (2020).
- [35] M. L. Mehta, *Random Matrices* (Academic, New York, 2004).
- [36] P. J. Forrester, *Log-Gases and Random Matrices* (LMS-34) (Princeton University Press, Princeton, NJ, 2010).
- [37] J. Wishart, *Biometrika* **20A**, 32 (1928).
- [38] A. G. Constantine, *Ann. Math. Stat.* **34**, 1270 (1963).
- [39] T. W. Anderson, *Ann. Math. Stat.* **34**, 122 (1963).
- [40] C. G. Khatri, *Ann. Math. Stat.* **35**, 1807 (1964).
- [41] R. J. Muirhead, *Aspects of Multivariate Statistical Theory* (Wiley, New York, 1982).
- [42] P. B. Slater, *J. Phys. A* **32**, 8231 (1999).
- [43] M. S. Byrd and P. B. Slater, *Phys. Lett. A* **283**, 152 (2001).
- [44] H.-J. Sommers and K. Życzkowski, *J. Phys. A* **36**, 10083 (2003).
- [45] I. Bengtsson, and K. Życzkowski, *Geometry of Quantum States: An Introduction to Quantum Entanglement* (Cambridge University Press, Cambridge, 2006).
- [46] V. A. Osipov, H.-J. Sommers, and K. Życzkowski, *J. Phys. A* **43**, 055302 (2010).
- [47] G. Borot and C. Nadal, *J. Phys. A* **45**, 075209 (2012).
- [48] X.-B. Hu and S.-H. Li, *J. Phys. A* **50**, 285201 (2017).
- [49] P. J. Forrester and S.-H. Li, *Int. Math. Res. Not.*, rnz028 (2019).
- [50] A. Sarkar and S. Kumar, *J. Phys. A* **52**, 295203 (2019).
- [51] P. J. Forrester and M. Kieburg, *Commun. Math. Phys.* **342**, 151 (2016).
- [52] M. Bertola, M. Gekhtman, and J. Szmigielski, *Commun. Math. Phys.* **287**, 983 (2009).
- [53] A. Uhlmann, *Rep. Math. Phys.* **9**, 273 (1976).
- [54] A. Uhlmann, *Groups and Related Topics*, edited by R. Gielera, J. Lukierski, and Z. Popowicz (Kluwer, Dordrecht, 1992).
- [55] A. Uhlmann, *Rep. Math. Phys.* **36**, 461 (1995).
- [56] M. Hubner, *Phys. Lett. A* **163**, 239 (1992).
- [57] M. Hubner, *Phys. Lett. A* **179**, 226 (1993).
- [58] J. Dittman, *J. Lie Theory* **3**, 73 (1993).
- [59] E. Bagan, A. Monras, and R. Muñoz-Tapia, *Phys. Rev. A* **71**, 062318 (2005).
- [60] R. Schmied, *J. Mod. Opt.* **63**, 1744 (2016).
- [61] R. Kueng and C. Ferrie, *New J. Phys.* **17**, 123013 (2015).
- [62] V. Madhok, C. A. Riofrio, and I. H. Deutsch, *Pramana* **87**, 65 (2016).
- [63] C. A. Fuchs and C. M. Caves, *Open. Syst. Inf. Dyn.* **3**, 345 (1995).
- [64] W. K. Wootters, *Phys. Rev. D* **23**, 357 (1981).
- [65] V. Vedral and M. B. Plenio, *Phys. Rev. A* **57**, 1619 (1998).
- [66] S. L. Braunstein and C. M. Caves, *Phys. Rev. Lett.* **72**, 3439 (1994).
- [67] L. Campos Venuti and P. Zanardi, *Phys. Rev. Lett.* **99**, 095701 (2007).
- [68] D. Šafránek, *Phys. Rev. A* **95**, 052320 (2017).
- [69] B. Aaronson, R. Lo Franco, and G. Adesso, *Phys. Rev. A* **88**, 012120 (2013).
- [70] T. R. Bromley, M. Cianciaruso, R. Lo Franco, and G. Adesso, *J. Phys. A* **47**, 405302 (2014).
- [71] V. Eremeev, N. Ciobanu, and M. Orszag, *Opt. Lett.* **39**, 2668 (2014).
- [72] J.-M. Gong, Q. Tang, Y.-H. Sun, and L. Qiao, *Phys. B (Amsterdam, Neth.)* **461**, 70 (2015).
- [73] M.-L. Hu and D.-P. Tian, *Ann. Phys. (NY)* **343**, 132 (2014).
- [74] M. Orszag, N. Ciobanu, R. Coto, and V. Eremeev, *J. Mod. Opt.* **62**, 593 (2015).
- [75] M. G. A. Paris, M. G. Genoni, N. Shammah, and B. Teklu, *Phys. Rev. A* **90**, 012104 (2014).
- [76] W. Roga, S. M. Giampaolo, and F. Illuminati, *J. Phys. A* **47**, 365301 (2014).
- [77] D. Spehner and M. Orszag, *New J. Phys.* **15**, 103001 (2013).
- [78] D. Spehner and M. Orszag, *J. Phys. A* **47**, 035302 (2014).
- [79] J. Emerson, Y. S. Weinstein, S. Lloyd, and D. G. Cory, *Phys. Rev. Lett* **89**, 284102 (2002).
- [80] L. Wei, *J. Phys. A* **53**, 235203 (2020).
- [81] L. Wei, *Phys. Rev. E* **102**, 062128 (2020).
- [82] R. Scharf, B. Dietz, M. Kuś, F. Haake, and M. V. Berry, *Europhys. Lett.* **5**, 383 (1988).
- [83] M. Kuś, J. Mostowski, and F. Haake, *J. Phys. A* **21**, L1073 (1988).
- [84] F. Haake and K. Życzkowski, *Phys. Rev. A* **42**, 1013(R) (1990).
- [85] K. Życzkowski, *J. Phys. A* **23**, 4427 (1990).
- [86] G. M. D'Ariano, L. R. Evangelista, and M. Saraceno, *Phys. Rev. A* **45**, 3646 (1992).
- [87] P. A. Miller and S. Sarkar, *Phys. Rev. E* **60**, 1542 (1999).
- [88] S. Chaudhury, A. Smith, B. E. Anderson, S. Ghose, and P. S. Jessen, *Nature (London)* **461**, 768 (2009).
- [89] H. Fujisaki, T. Miyadera, and A. Tanaka, *Phys. Rev. E* **67**, 066201 (2003).
- [90] M. Kumari, E. Martin-Martinez, A. Kempf, and S. Ghose, [arXiv:1711.07906](https://arxiv.org/abs/1711.07906).
- [91] M. Kumari and S. Ghose, *Phys. Rev. E* **97**, 052209 (2018).
- [92] M. Kumari and S. Ghose, *Phys. Rev. A* **99**, 042311 (2019).
- [93] V. Madhok, V. Gupta, D.-A. Trotter, and S. Ghose, *Phys. Rev. E* **91**, 032906 (2015).
- [94] X. Wang, S. Ghose, B. C. Sanders, and B. Hu, *Phys. Rev. E* **70**, 016217 (2004).
- [95] C. M. Trail, V. Madhok, and I. H. Deutsch, *Phys. Rev. E* **78**, 046211 (2008).
- [96] A. Lakshminarayan, *Phys. Rev. E* **64**, 036207 (2001).
- [97] J. N. Bandyopadhyay and A. Lakshminarayan, *Phys. Rev. E* **69**, 016201 (2004).
- [98] J. N. Bandyopadhyay and A. Lakshminarayan, *Phys. Rev. Lett.* **89**, 060402 (2002).
- [99] Ph. Jacquod, *Phys. Rev. Lett.* **92**, 150403 (2004).
- [100] C. Petitjean and Ph. Jacquod, *Phys. Rev. Lett.* **97**, 194103 (2006).
- [101] M. Znidaric and T. Prosen, *J. Phys. A* **36**, 2463 (2003).
- [102] A. Tanaka, H. Fujisaki, and T. Miyadera, *Phys. Rev. E* **66**, 045201(R) (2002).

- [103] R. Demkowicz-Dobrzański and M. Kuś, *Phys. Rev. E* **70**, 066216 (2004).
- [104] S. Kumar, B. Sambasivam, and S. Anand, *J. Phys. A* **50**, 345201 (2017).
- [105] H. Kubotani, S. Adachi, and M. Toda, *Phys. Rev. Lett.* **100**, 240501 (2008).
- [106] M. Znidaric, *J. Phys. A* **40**, F105 (2007).
- [107] H. Kubotani, S. Adachi, and M. Toda, *Phys. Rev. E* **87**, 062921 (2013).
- [108] S. Tomsovic, A. Lakshminarayan, S. C. L. Srivastava, and A. Bäcker, *Phys. Rev. E* **98**, 032209 (2018).
- [109] Y. Y. Atas, E. Bogomolny, O. Giraud, and G. Roux, *Phys. Rev. Lett.* **110**, 084101 (2013).
- [110] Y. Y. Atas, E. Bogomolny, O. Giraud, P. Vivo, and E. Vivo, *J. Phys. A* **46**, 355204 (2013).
- [111] V. Oganesyan and D. A. Huse, *Phys. Rev. B* **75**, 155111 (2007).
- [112] V. Oganesyan, A. Pal, and D. A. Huse, *Phys. Rev. B* **80**, 115104 (2009).
- [113] A. Pal and D. A. Huse, *Phys. Rev. B* **82**, 174411 (2010).
- [114] M. Collura, H. Aufderheide, G. Roux, and D. Karevski, *Phys. Rev. A* **86**, 013615 (2012).
- [115] S. Iyer, V. Oganesyan, G. Refael, and D. A. Huse, *Phys. Rev. B* **87**, 134202 (2013).
- [116] N. D. Chavda and V. K. B. Kota, *Phys. Lett. A* **377**, 3009 (2013).
- [117] N. D. Chavda, H. N. Deota, and V. K. B. Kota, *Phys. Lett. A* **378**, 3012 (2014).
- [118] K. Roy, B. Chakrabarti, N. D. Chavda, V. K. B. Kota, M. L. Lekela, and G. J. Rampho, *Europhys. Lett.* **118**, 46003 (2017).
- [119] S. H. Tekur, S. Kumar, and M. S. Santhanam, *Phys. Rev. E* **97**, 062212 (2018).
- [120] S. H. Tekur, U. T. Bhosale, and M. S. Santhanam, *Phys. Rev. B* **98**, 104305 (2018).
- [121] A. M. García-García, T. Nosaka, D. Rosa, and J. J. M. Verbaarschot, *Phys. Rev. D* **100**, 026002 (2019).
- [122] A. Sarkar, M. Kothiyal, and S. Kumar, *Phys. Rev. E* **101**, 012216 (2020).
- [123] T. A. Brody, J. Flores, J. B. French, P. A. Mello, A. Pandey, and S. S. M. Wong, *Rev. Mod. Phys.* **53**, 385 (1981).
- [124] A. P. Prudnikov, Y. A. Brychkov, and O. I. Marichev, *Integrals and Series: Inverse Laplace Transforms*, Vol. 5 (Gordon and Breach, London, 1992).
- [125] O. Bohigas, M. J. Giannoni, and C. Schmit, *Phys. Rev. Lett.* **52**, 1 (1984).
- [126] T. Guhr, A. Müller-Groeling, and H. A. Weidenmüller, *Phys. Rep.* **299**, 189 (1998).
- [127] S. Kumar, *Europhys. Lett.* **101**, 20002 (2013).
- [128] J. Emerson, Y. Weinstein, M. Saraceno, S. Lloyd, and D. Cory, *Science* **302**, 2098 (2003).
- [129] A. Ambainis and J. Emerson, in *Proceedings of the 22nd Annual IEEE Conference on Computational Complexity* (IEEE Computer Society Press, Los Alamitos, CA, 2007), pp. 129–140.
- [130] D. Gross, K. Audenaert, and J. Eisert, *J. Math. Phys.* **48**, 052104 (2007).
- [131] C. Dankert, R. Cleve, J. Emerson, and E. Livine, *Phys. Rev. A* **80**, 012304 (2009).
- [132] F. G. S. L. Brandão, A. W. Harrow, and M. Horodecki, *Phys. Rev. Lett.* **116**, 170502 (2016).
- [133] F. G. S. L. Brandão, A. W. Harrow, and M. Horodecki, *Commun. Math. Phys.* **346**, 397 (2016).
- [134] A. P. Prudnikov, Y. A. Brychkov, and O. I. Marichev, *Integrals and Series: More Special Functions*, Vol. 3 (Gordon and Breach, London 1990).